

The Extraction and Characterisation of Chitin and Chitosan from Six Species of Beetles: Demonstrate That Beetles Are a Valuable Source of These Biopolymers

¹Sahana Savappla Anand, ²Sanjana Shajan, ²Neerkaje Subrayabhat Devaki, ¹Shakuntala Venkat* and ²Honnagondanahally Channaveerappa

Author's Affiliation:

¹Department of Studies in Zoology, Manasagangotri, University of Mysore, Mysuru-570006, India

²Department of Molecular Biology, Yuvaraja's College (Autonomous and a Constituent College of University of Mysore), University of Mysore, Mysuru-570 005, India.

***Corresponding author:**

Shakuntala Venkat,

Department of Studies in Zoology, Manasagangotri, University of Mysore, Mysuru-570006, India

E-mail: drshakunthalav2@gmail.com

Received on 18.03.2025

Revised on 27.06.2025

Accepted on 15.07.2025

ABSTRACT:

This work aimed to extract chitin and chitosan from the exoskeletons of different beetle species and to analyze the properties of chitin and its derivative, chitosan. Chitosan is increasingly acknowledged as a significant primary material for producing a variety of products. Annually, the demand for chitin derivatives increases. To meet this requirement, it becomes imminent to seek novel sources of chitin. This study investigates many beetle species as prospective chitin sources for chitosan synthesis. The chitin content obtained from the dry weight of beetle raw material varied between 7.2% and 42.2%. The extraction percentages of chitosan differed among species, ranging from 13.5% to 89.2% of the chitin weight removed. The XRD analysis of chitin exhibited prominent peaks at 9.2 degrees, 19.2 degrees, 22.8 degrees, and 26.3 degrees. The X-ray diffraction (XRD) patterns of chitosan obtained from six different beetle species exhibit significant peaks at around 8.9°, 20.1°, 25.3°, and 26.5°. The crystallinity index of chitin ranges from 22% to 55%, whereas chitosan exhibits a range of 8.5% to 13.4%; nevertheless, the degree of deacetylation (DDA) of chitosan consistently exceeds 69% across all species. The FTIR spectra of chitin and chitosan from each species exhibited significant variations in the amide III, amide II, and amide I regions. The SEM images of chitin/chitosan from these insects exhibited a combination of flake-shaped structures, nanopores, and nanofibers. The findings indicate that the extraction of chitin and chitosan from beetle exoskeletons is an uncomplicated process that yields a significant amount of these polymers. Chitin and chitosan exhibited SEM-documented morphologies characterized by a reduced number of pores and an increased presence of fibers. The structural analysis has confirmed that the chitin in these species is exclusively in the alpha form. These species serve as exceptional reservoirs of chitin and chitosan.

Keywords:

Chitin extraction, chitosan yield, characterization, band patterns, scarabid beetles, chitosan source, crystallinity index.

How to cite this article: Sahana SA, Sanjana Shajan, NS Devaki, Shkunthala V, and Channaveerappa H (2025). The Extraction and Characterisation of Chitin and Chitosan from Six Species of Beetles: Demonstrate That Beetles Are a Valuable Source of These Biopolymers. *Bulletin of Pure and Applied Sciences-Zoology*, 44A (2), 96-117.

INTRODUCTION

Chitin is a naturally occurring, abundant, linear polysaccharide made up of N-acetyl-D-glucosamine monomers that are connected by β -1,4-glycosidic bonds. Chitosan, a copolymer formed of glucosamine and N-acetyl glucosamine, is derived from chitin through the process of deacetylation and which is the subject of the majority of studies aimed at quantifying and characterizing the resulting chitosan. Chitosan is becoming a valuable raw material for producing a wide variety of products used in food, medical, pharmaceutical, healthcare, agriculture, industry, and environmental pollution protection applications. Chitin, the precursor of chitosan, is a biopolymer found in various organisms, including crustacean and mollusk exoskeletons, algae, fungal cell walls, and insects. The chitin content differs among these organisms: in crab cuticles, it ranges from 15–30%; in crustacean exoskeletons, it varies from 20–30% (Yeul and Rayulu 2012); in shrimp, it ranges from about 5–25%; in insect cuticles, it ranges from 5–25% (Abidin et al., 2020); in fungal cell walls, it ranges from 2–44%. In search of alternative sources for chitin, insects are found to be valuable sources because their exoskeleton is comprised of nearly 40% chitin (Hanh et al., 2020). Each year the demand for chitin derivatives particularly chitosan, is increasing (Pellis et al., 2022), to meet this requirement additional sources of chitin are continuously being explored. In this work, we have examined different species of beetles as sources for extracting chitin and its conversion into chitosan. Beetles form the largest order among the class of insecta, comprising 350,000 species and 23,000 genera around the world. It is estimated that the species of beetles are more than vascular plants or fungi and 90 times more than the mammal species existing (Klimaszewski and Watt, 1997). This underscores the significance of these insects being examined for their utility as the biological source of chitin. Over the past twenty years, there has been a lot of research done on the possible common uses of chitin and its derivatives, primarily chitosan. A number of authors have addressed the issue of removing chitin from its natural sources and deacetylating

it to produce the far more valuable substance chitosan (Dahmane et al., 2014; Hajji et al., 2014; Kumari et al., 2015; El Knidri et al., 2018; Yadav et al., 2019; Varma and Vasudevan, 2020; Vino et al., 2012; Uğurlu and Duysak, 2022). Interest in insects as a source of valuable biologically active substances has significantly increased over the past few years. (Klimaszewski and Watt, 1997). Depending on the anatomical location, developmental stage, and physiological function of the organ, the chitin in insect cuticles varies greatly in both nature and organization (Elkadaoui et al., 2024). The serosal cuticle covering the developing embryo, larvae, pupae, and adults, as well as the cuticles connected to adult components like the pronotum, forewing, and hindwing, all have distinctly different characteristics, in beetles. When a beetle reaches adulthood, its cuticle thickens and deposits layers of cuticular material along with chitin that are structurally and mechanically separate from those that were deposited before adult emergence (Muthukrishnan et al., 2020).

Chitin can be found in the α , β -, and γ -forms; the differences among these depend on the arrangement of chains in the crystalline regions (Jang et al., 2004). In most cases, the crystallinity index provides information about the crystal state, but it is also very useful for distinguishing α -chitin from β -chitin. The crystallinity index (CI) can also be calculated on the basis of X-ray diffractograms. FTIR ascertains the molecular structure by absorbing infrared spectra from different functional groups of chitin and chitosan molecules, producing characteristic wavelengths. The deacetylation of the two macromolecules enables this property. The partially deacetylated form of chitin, - the chitosan, is obtained by converting some of the N-acetyl-D-glucosamine into D-glucosamine. The degree of deacetylation in chitosan is defined as the ratio of D-glucosamine to N-acetyl-D-glucosamine. In nature, chitin is neither entirely acetylated nor totally deacetylated. The only cationic polymer found in nature is chitosan (Rinaudo, 2006). Chitosan has a wide range of applications in several fields due to its biodegradability, biocompatibility, and non-toxicity (Vino et al., 2012; Varma and Vasudevan, 2020). We present here, the findings

of the current study on six species of beetles, which involved the chemical extraction of chitin and chitosan from their exoskeleton, followed by characterization through XRD, FTIR, and SEM analysis.

MATERIAL AND METHODS

Chitin extraction was conducted using six species of beetles. We caught four species of beetles, *Oryctus rhinoceros* (Coleoptera:Scarabaeidae), *Lanelater Arnett* species (Coleoptera:Elateridae), *Anamola bengalensis* (Coleoptera:Scarabaeidae), and *Holotrichia serrata* (Coleoptera:Scarabaeidae), from the Manasagangothri campus of the University of Mysore. We collected two species, *Abscondita perplexa* (Coleoptera: Lampyridae) and *Anamola varicolor* (Coleoptera: Scarabidae), from agricultural fields in Alur, Davanagere. For further processing, we preserved the collected beetles as dry specimens in a deep freezer.

Preparation of raw material

The beetles were dissected open to clear the internal contents and then in a hot air oven (Ascension Innovations, J.J. Biotek) at 100 °C for about 4-5 hours until they were completely dry; later, those were scraped to remove internal debris and retained only the chitinous exoskeleton and elytra. The exoskeletal content was ground to a fine powder using a pestle and mortar. The initial weight of the ground powder was recorded with the help of a digital balance. The material was subsequently used for chitin extraction.

Extraction of chitin

The chitin and chitosan were extracted from the powdered raw material of the insect's exoskeleton through demineralization and deproteinization processes. Demineralization was carried out by treating the raw material with a 1 M HCl solution at room temperature with a solution-to-solid ratio of 15 mL/gm overnight. The resulting solid fraction was washed with distilled water until a neutral pH was achieved. Deproteinization was done using alkaline treatment with 1.0 M sodium hydroxide at 100°C for 4 hours. {NaOH -1:10(g/ml)}.The resulting chitin was then washed with distilled water to neutralize it. The purified chitin was dried in a

hot air oven. The chitin content was weighed and stored for further analysis.

Chitosan preparation

The chitin isolated from each sample was subjected to treatment with 50% NaOH (15 mL/g) at a temperature of 100 °C for a duration of 8 hours. The liquid was agitated periodically to ensure a uniform reaction. Following the filtration process, the remaining substance was thoroughly rinsed with distilled water multiple times until it reached a neutral pH. The chitosan was dried in a vacuum oven at a temperature of 50 degrees Celsius for a duration of 24 hours. The chitosan samples underwent purification by dissolving them in a 2% acetic acid solution and subsequently re-precipitating them in a 20% NaOH solution. The samples were subsequently rinsed with distilled water until a neutral pH was reached and then subjected to freeze-drying.

Estimating the Quantity of chitin and Chitosan.

The amount of extracted chitin and chitosan is calculated by using the following formula (Triunfo *et al.*,2022)

$$\begin{aligned} \text{Chitin yield (\%)} &= \frac{\text{dry weight of chitin (g)}}{\text{dry weight of raw insect sample(g)}} \times 100 \\ \text{Chitosan yield (\%)} &= \frac{\text{dry weight of chitosan(g)}}{\text{dry weight of raw insect sample(g)}} \times 100 \end{aligned}$$

X-ray diffraction (XRD) analysis

X-ray diffraction is employed to determine the degree of crystallinity of the extracted chitin and chitosan obtained from six distinct beetles. The Rigaku Smart lab, a powder diffractometer manufactured in Japan, is utilized for X-ray diffraction (XRD) experiments. The software OriginPro 2024 is utilized for generating graphical representations based on acquired data.

Fourier-transform infrared spectroscopy (FTIR)

The chitin and chitosan samples were analyzed using ATR (Attenuated Total Reflectance) Fourier-transform infrared spectrophotometry in the range of 4,000 to 400 cm⁻¹. The analysis was performed using the PerkinElmer Spectrum instrument, provided by PIKE Technology Ltd. We utilized commercially sourced chitin derived

The Extraction and Characterisation of Chitin and Chitosan from Six Species of Beetles: Demonstrate That Beetles Are a Valuable Source of These Biopolymers

from shrimp as a standard to evaluate and compare our findings.

Crystallinity index and Degree of deacetylation:

The crystallinity index was calculated using the formula-

$$\text{Crystallinity index (\%)} = \frac{\text{Area of crystalline peaks}}{\text{Area of all peaks (crystalline + Amorphous)}} \times 100$$

The degree of deacetylation of chitosan is determined using the formula provided by Lavertu et al. (2003) and Sen et al. (2016).

$$\text{DDA} = 100 - \text{DA}$$

$$\text{Where DA\%} = [A1320/A1420 - 0.3822] / 0.03133$$

Scanning Electron Microscopy (SEM)

The surface morphology of extracted chitin and chitosan was analyzed using a Hitachi, JSM-6700F scanning electron microscope from Japan, following the procedure outlined by Kavya et al (2018)[21]. The desiccated chitin and chitosan powder samples were affixed to adhesive tape on a holder stub and subsequently covered with a thin layer of gold using a sputter coater. These samples were then scanned to obtain pictures.

RESULTS

To obtain chitin, the basic ingredient required, we crushed the dried exoskeletons of six different species of beetles. The amount of dehydrated raw material used for chitin extraction varied from 0.122 grams of *Abscondita perplexa* to 4.053 grams of *Anomala bengalensis* at its highest weight. The chitin contents recovered from the six species of beetles varied from 21.0% in *Holotrichia serrata* to 37.7% in *Anomala bengalensis* (Table 1). Chitosan is derived from chitin by the processes of demineralization and deproteinization. The chitosan percentage was estimated using two different methods: one based on the initial dry weight of the material, and the other based on the weight of the extracted chitin. This percentage differed among the six species. The lowest amount of 4.05% to its dry weight, equivalent to 4.053 grams, was found in *Anomala bengalensis*, while the highest

amount of 20.49% to its dry weight, equivalent to 0.122 grams, was reported in *Abscondita perplexa*. The chitosan yield for the other four species to their dry weight ranged from 4.53% to 14.93%. The percentage deviation of chitosan, relative to the amount of chitin extracted, exhibited a significant range of variance. The high percentage recorded was 89.2% in *Abscondita perplexa*, while the lowest was 13.5% in *Anomala varicolor* (Table.1).

Six different species of beetles' surface morphologies of chitin and chitosan were investigated using scanning electron microscopy analysis. It was observed that the chitin/chitosan extracted from these insects consisted of flake-shaped structures, nanopores, and nanofibers that were either dispersed or aggregated with other chitin or chitosan constituents. The chitin in *Oryctus rhinoceros* (Fig. 1A) displayed a morphology resembling flakes, characterized by a depressed and rough surface. The nanofibrillar structures of chitin have an irregular form either are found scattered or found associated with flakes. The chitin of *Abscondita perplexa* (fig.1B) exhibited a smooth laminar structure that was occasionally interrupted by sparsely distributed nanopores and nano fibers. The primary constituents of chitin in *Lanelater* species were rough-surfaced, flake-like structures; these constituents allowed irregular nanofibers linked to the flakes' lamellar structures to be seen. (Fig.1.C). The chitin structure of *Holotrichia serrata* (Fig.1 D&E) was more complicated with entangled nanofibres laid between smooth surface flakes. The nanofibres were irregularly placed. In *Anomala bengalensis* the chitin structure (fig.1 F) was composed of small flake like structures, some with rough and a few with smooth surfaces. The rough surfaced flakes were smaller in size than the smooth flakes. The nano fibrous structures were indistinct both in size and organization. In *Anomala varicolor* (fig. 1 G &H), we found flakes with depression and distinct, scattered nanofibres in the organization of chitin.

Table 1: Showing the percent of chitosan and chitosan yield by six beetle species.

Species name	Dry weight of raw insect sample (in gm)	The final weight of chitin obtained (in gm)	The final weight of chitosan obtained (in gm)	% of chitin yield obtained	% of chitosan yield to its dry weight	% of chitosan yield to its chitin extracted
<i>Oryctes rhinoceros</i>	2.612	0.938	0.390	35.9%	14%	41.5%
<i>Abscondita perplexa</i>	0.122	0.028	0.025	22.9%	20%	89.2%
<i>Lanelater species</i>	0.716	0.238	0.053	33.2%	7.4%	22%
<i>Holotrichia serrate</i>	0.50	0.105	0.028	21%	5.6%	26%
<i>Anomala bengalensis</i>	4.053	1.530	0.382	37.7%	9.4%	24.9%
<i>Anomala varicolor</i>	2.295	0.765	0.104	33.3%	4.5%	13%

The SEM images of chitosan in six species of beetles had flake like appearance in all the species but the nature of these flakes varied from species to species. In *Oryctes rhinoceros* (fig. 2 A) the chitosan chips were lamina like formed of irregular short nanofibres. On these structures one to two small nanopores were also seen but these pores are less prominent. In *Abscondita perplexa* (fig 2 B) the porous nature of chitosan is prominent, the nanofibres are arranged in bundles, the pores are almost evenly distributed. In *Holotrichia serrate* (fig. 2 D) the chitosan formed of closely packed porous nano fibres. The nano pores are scattered on the surface of flat chitosan flakes. The chitosan topology of *Lanelater species* (fig.2 C) slightly distinct, formed of fragmented lamina of irregular size and shape, unlike in other species the fibres are indistinct and short. In *Anomala bengalensis* (fig.2 E) the chitosan is arranged in the form of thick bundles of nanofibres. These fibres run parallel to each other to form thin chips of smooth chitosan. In *Anomala varicolor* (fig.2 F) the chitosan was represented as irregular flakes of uneven shapes, and the nanofibers were present

as thick bundles of different shapes. Some of the chitosan flakes had a central depression.

X-ray diffraction (XRD) conducted to ascertain the degree of crystallinity in chitin and chitosan from six different species of beetles (see Table 2). The chitin of *Oryctes rhinoceros* exhibited two prominent peaks at 9.2°, 19.2°, 22.8°, 26.3° (Fig.3 A) and had a crystallinity of 42%. The soft-bodied firefly or bioluminescent beetle *Abscondita perplexa* (Figure 3 B) displayed high peaks at 9.2°, 19.2°, 24.1°, 26.22° degrees, with a crystallinity index (C I) of 23%. Similarly, the click beetle *Lanelater species* (Figure 3 C) exhibited significant peaks at 9.2°, 19.3°, 23.5°, 26.5° and had a crystallinity index of 67%. *Holotrichia serrata* (Figure 3D) displayed high peaks at 9.2°, 19.3°, 23.6°, 26.3° degrees and had a crystallinity of 55%. *Anomala bengalensis* and *Anomala varicolor* also exhibited high peaks at (Figure 3E) 9.2°, 19.3°, 23°, and 26.5°, with a crystallinity of 45% (Figure 3F) and the degree of crystallinity was measured at 8.7°, 20°, 23°, and 26.30°, crystallinity index values of 22% respectively.

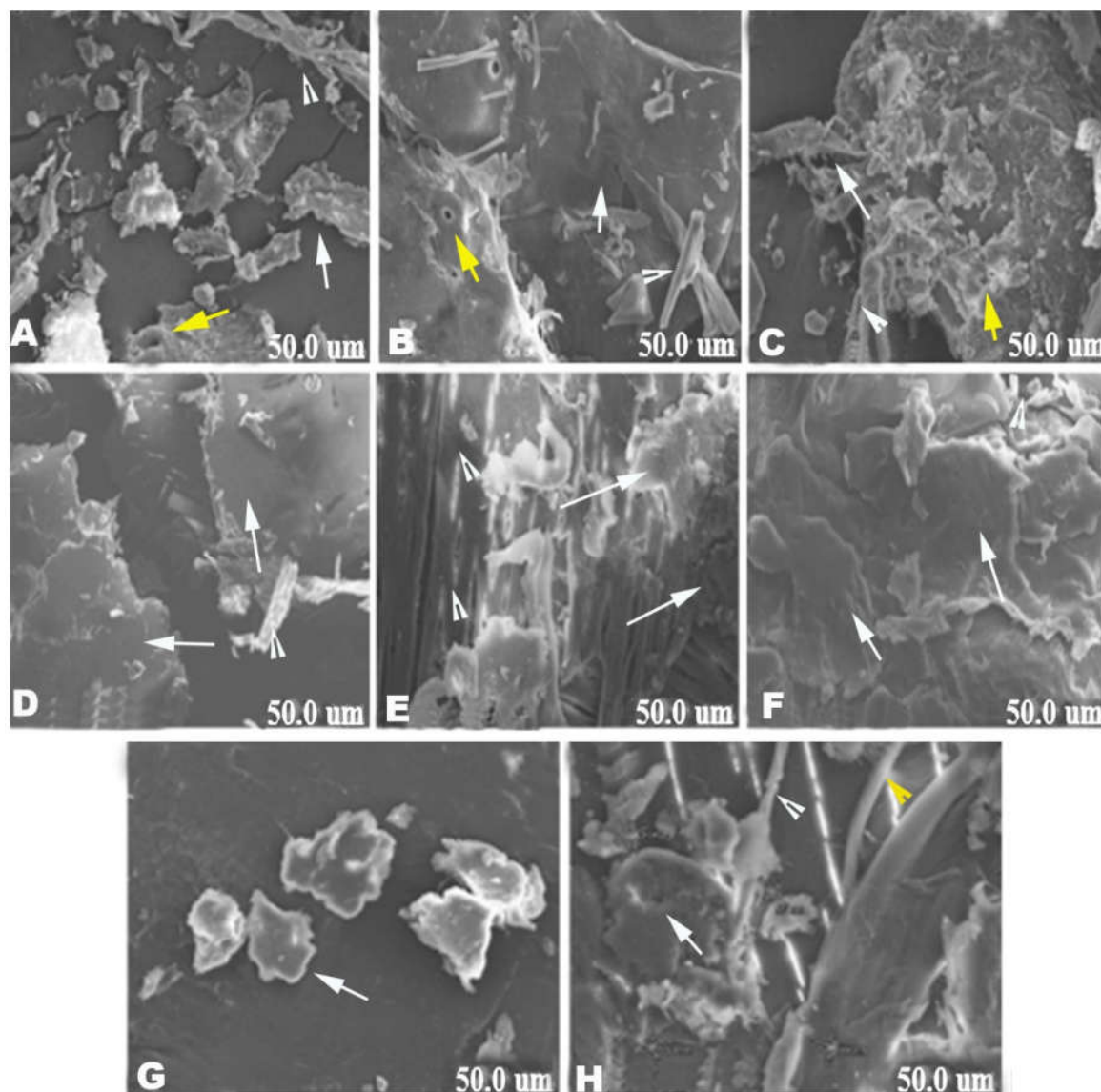


Figure 1: SEM images of extracted chitin from A. *Oryctes rhinoceros* B, *Abscondita perplexa* C, *Lanelater species* D&E, *Holotrichia serreta* , F *Anomala bengalensis* and G&H *Anomala varicolor* , .*(white arrow-flakes, yellow arrow-nano pores, arrow head pointer-Nano fibers) *common to all images, missing indicator in the image means- structure not found.

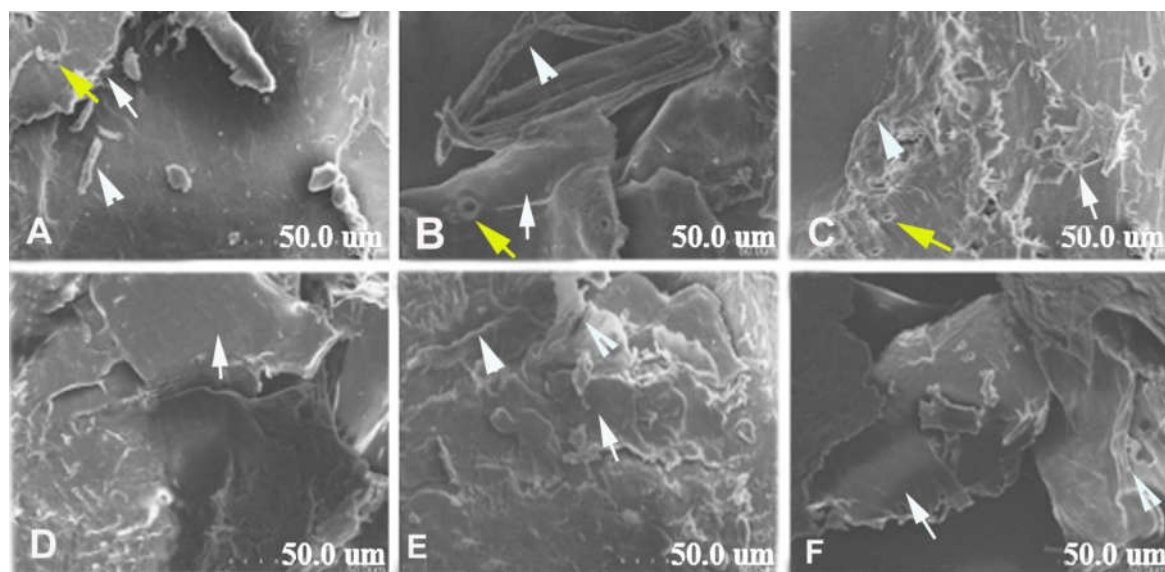


Figure 2: SEM images of extraced chitosan from A *Oryctes rhinoceros*, B. *Abscondita perplexa* ,C, *Lanelater species*, D. *Holotrichia serrata* ,E. *Anomala bengalensis* and F. *Anomala varicolor* .*(white arrow-flakes, yellow arrow-nano pores,arrow head pointer-Nano fibers)*common to all images, missing indicator in the image means- structure not found

Table 2: Showing peak 2- value and crystallinity index (%) of chitin from six different species.

Species	<i>Oryctes rhinoceros</i>	<i>Abscondita perplexa</i>	<i>Lanelater species</i>	<i>Holotrichia serrata</i>	<i>Anomala bengalensis</i>	<i>Anomala varicolor</i>
Peak 2	9.2,19.2, 22.8,26.3	8.12,19.2, 24.1,26.2	9.1,19.3, 22.8,26.5	9.2,19.3,26.3	9.2,19.3, 23,26.5	8.7,20, 23,26.3
Crystallinity Index (%)	42%	23%	67%	55%	45%	22%

Table 3: Showing peak 2 value and crystallinity index (%) of chitosan from six different species.

Species	<i>Oryctes rhinoceros</i>	<i>Abscondita perplexa</i>	<i>Lanelater species</i>	<i>Holotrichia serrata</i>	<i>Anomala bengalensis</i>	<i>Anomala varicolor</i>
Peak 2	9.4,20.1, 22.9,26.3	9.1,20.2, 26.4,28.7	8.9,20.1, 26.5	8.9,20.4, 27.3,30.5	9.5,20.1,26.5,	9.1,20.3, 26.4
Crystallinity Index (%)	9.5%	11%	14%	11.1%	8.5%	13.4%

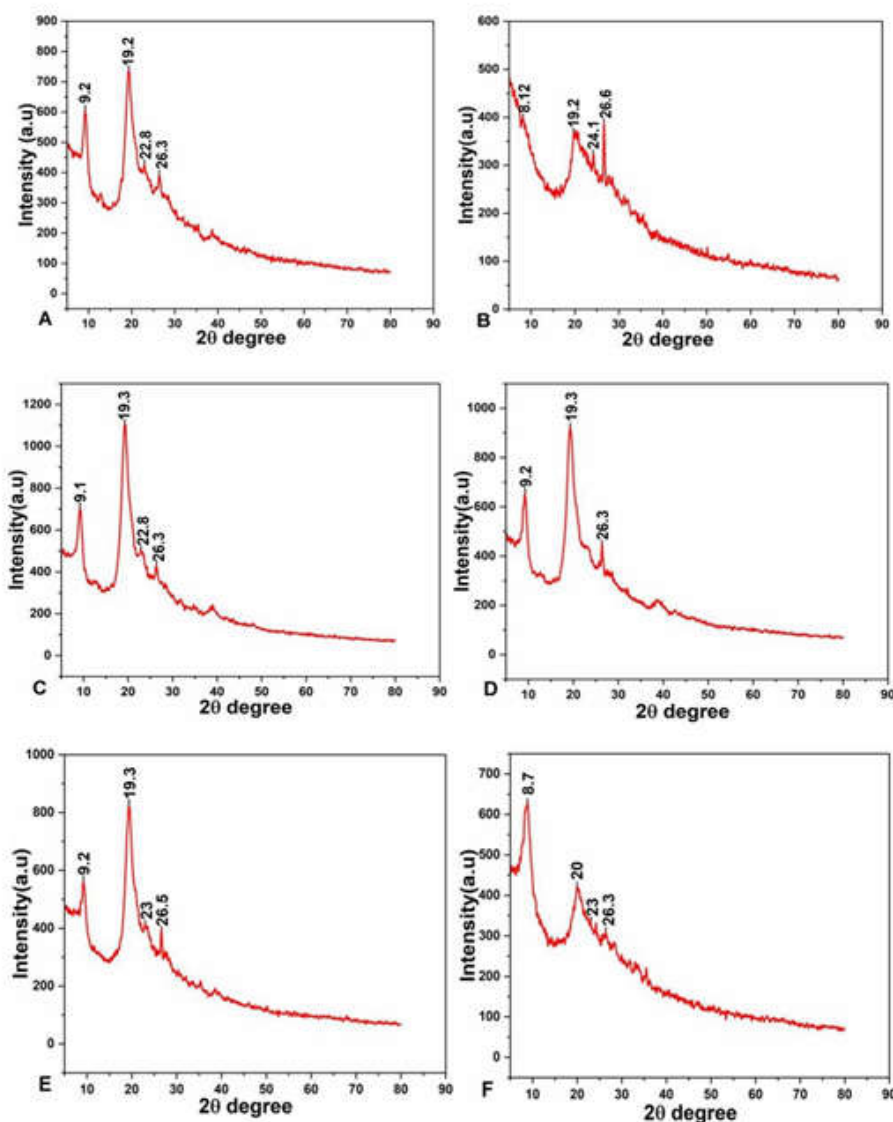


Figure 3: XRD patterns of chitin from six species of beetles A. *Oryctes rhinoceros* , B. *Abscondita perplexa* C. *Lanelater species*, D. *Holotrichia serrata*, E. *Anomala bengalensis*, and F. *Anomala varicolor*

XRD patterns of chitosan obtained for six species of beetles are represented in figure. (4) (Table. 3). The chitosan of *Oryctes rhinoceros* (Figure. 4A) produced three peaks at 9.4°, 20.1°, 26.3°, the crystalline index was 9.5%, chitosan of *Abscondita perplexa* (Figure. 4B) had four bands of which two were strong peaks 9.1°, 20.2°, 26.4°, 28.7° the crystallinity index was 11% , *Lanelater species* (Figure. 4C) generated two

strong peaks and two strong peaks at 8.9°, 20.1°, 25.3°, 26.5° its CI was 14%, *Holotrichia serrata* (Figure. 4D) produced peaks at 8.9°, 20.4°, 27.3°, 30.5° with CI 11.1%, *Anomala bengalensis* (Figure. 4E) had peaks at 9.5°, 20.1°, 26.5° and its CI was 8.5%) *Anomala varicolor* (Figure. 4F) peaks were found at 9.1°, 20.3°, 26.4°, 28.6° , with CI 13.4% .

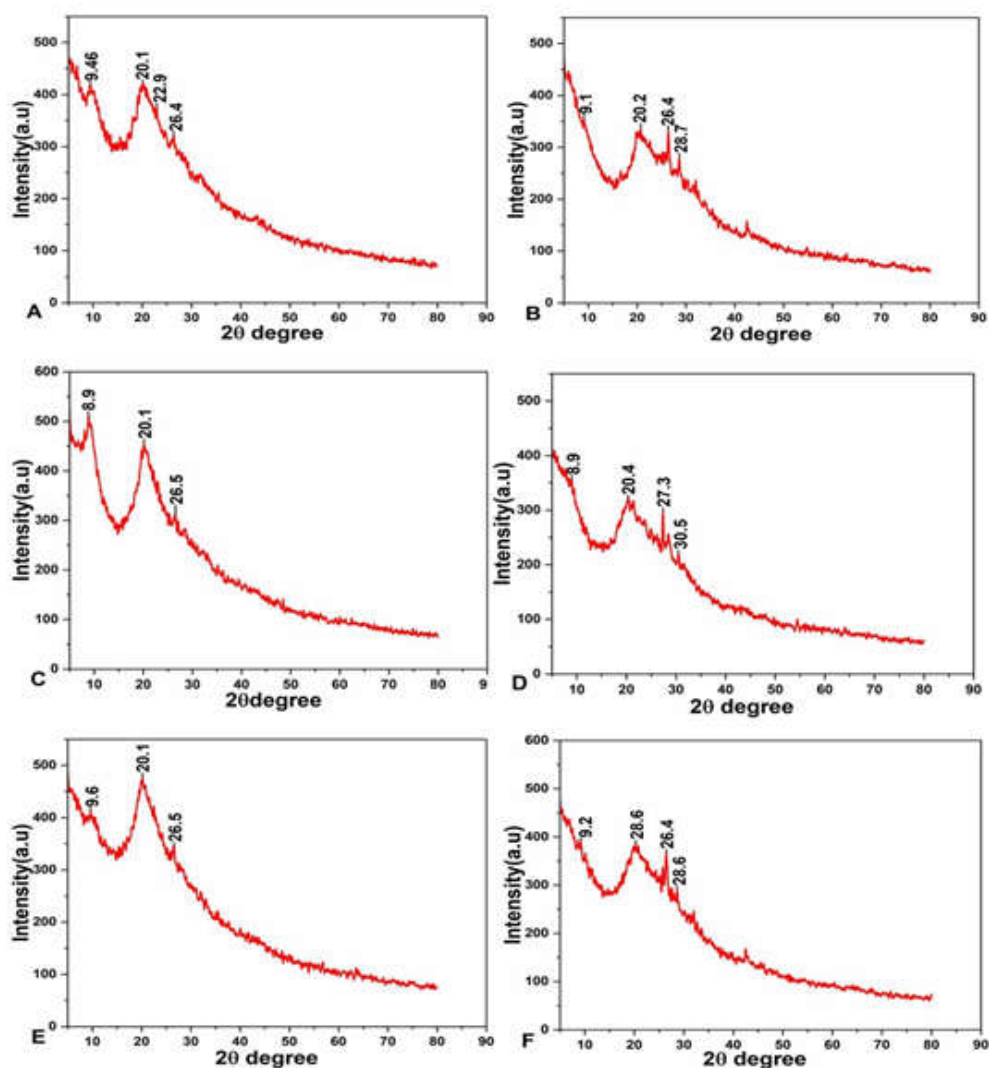


Figure 4: XRD patterns of chitosan from six species of beetles (A) *Oryctes rhinoceros*, (B) *Abscondita perplexa*, (C) *Lanelater species*, (D) *Holotrichia serrata*, (E) *Anomala bengalensis*, and (F) *Anomala*

FTIR analysis was performed to determine the material composition of the chitin and chitosan samples. For chitin, we used the characteristic wavelength of O-H stretching, 3439, as the standard. In the same area, the wave lengths were 3447 for *Oryctes rhinoceros* (Fig. 5A) and 3439 for *Abscondita perplexa* (Fig. 5B). For N-H stretch, the wave lengths that created were 3268, 3257, 3260, 3270, 3266, 3264, 3266; for Amide I band length 1631, 1654, 1650, 1655, 1651, 1663; and for Amide II band length 1550, 1554, 1546, 1575, 1553, and 1568, these were the wave length

frequencies for *Oryctes rhinoceros*, *Abscondita perplexa*, *Lanelater species* (Fig.5C), *Holotrichia serrata*, (Fig.5D) *Anomala bengalensis*, (Fig.5E) and *Anomala varicolor* (Fig.5F), on the other hand. Vibrational modes of OH out-of-plane bending, NH out-of-plane bending, ring stretching, CH₃ wagging along chains, CO stretching, asymmetric in-phase ring stretching mode, CH₂ bending, and CH₃ deformation have been identified for all six species, and a standard for each of these criteria is presented in the table (4).

The Extraction and Characterisation of Chitin and Chitosan from Six Species of Beetles: Demonstrate That Beetles Are a Valuable Source of These Biopolymers

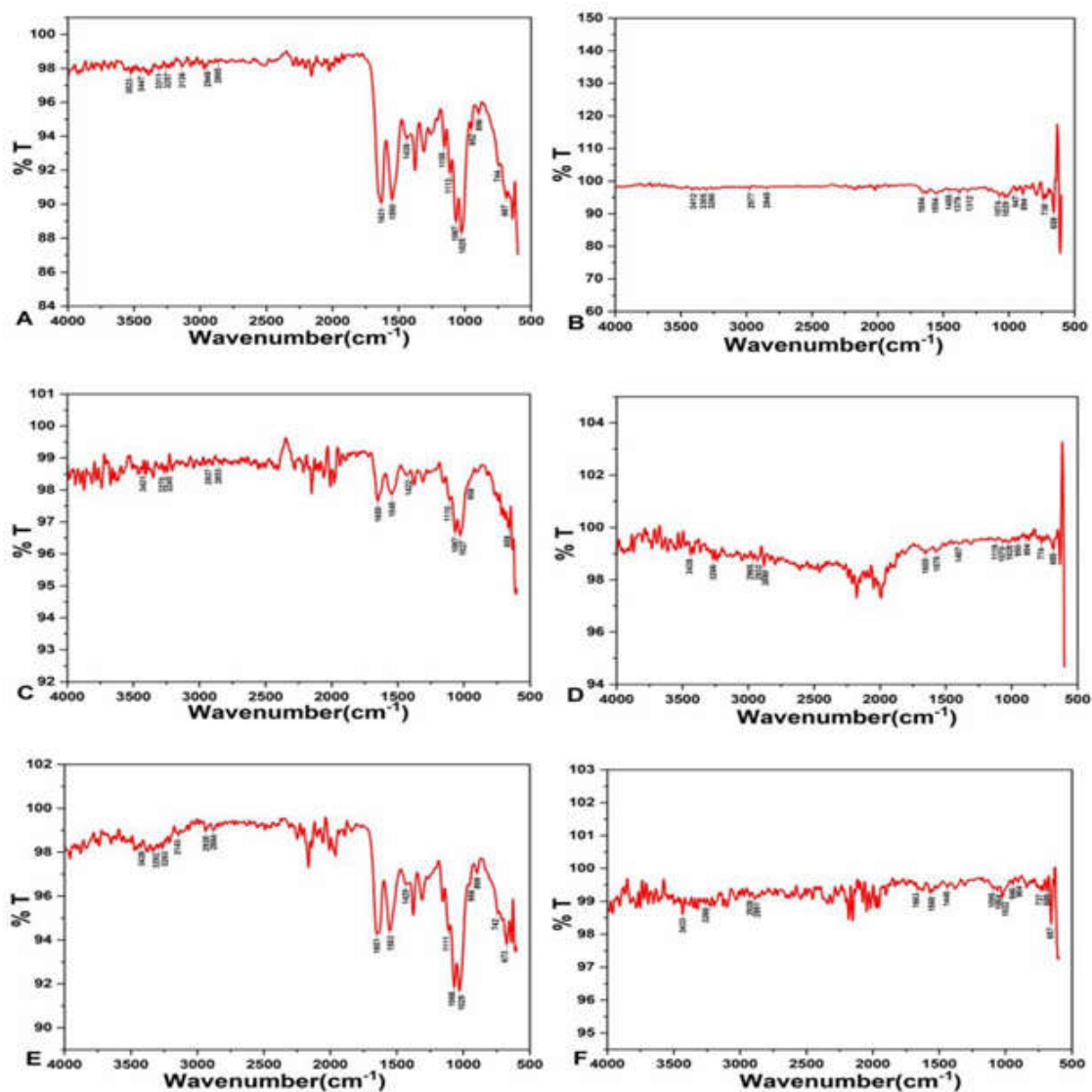


Figure 5: FT-IR spectra of chitin from A. *Oryctus rhinoceros*, B. *Abscondita perplexa*, C. *Lanelater species*, D. *Holotrichia serrata*, E. *Anamola bengalensis*, F. *Anamola varicolor*

Table (5) presents a comparison of the functional groups of chitin isolated from different species of beetles with conventional chitin. The spectral wavelength of the functional OH group was measured to be 3448, 3523, 3412, 3431, 3459, 3426, and 3433, from beetles *Oryctus rhinoceros*, *Abscondita perplexa*, *Lanelater species*, *Holotrichia serrata*, *Anomala bengalensis*, *Anomala varicolor* and the N-H stretching of the functional OH group in chitin produced a spectral wavelength

range of 3300–3250, with specific peaks at 3311, 3305, 3245–3299, 3266, 3264–3292, and 3266, as well as a peak at 2891–2901 by chitin of the beetle species in the mentioned order. The spectra for C-H stretching ranged from 2891 to 2901. The N-H bending and C-O stretching were seen in relation to the N-H bending. The wavelengths corresponding to the CH₃, C-O-C, and N-H groups are listed in Table 5.

Table 4: Functional groups of extracted chitin from different beetles compared to commercial standard chitin

Groups	Wavelength(cm ⁻¹)						
	Standard chitin *	<i>Oryctes rhinoceros</i>	<i>Abscondita perplexa</i>	<i>Lanelater species</i>	<i>Holotrichia serrata</i>	<i>Anomala Bengalensis</i>	<i>Anomala varicolor</i>
OH	3448	3523	3412	3431	3459	3426	3433
N-H stretching	3300-3250	3311	3305	3245-3299	3266	3264-3292	3266
C-H stretching	2891	2865	2865	2901	2880	2884	2891
C = O stretching	1680-1660	1631	1654	1650	1655	1651	1663
N-H bending	1560-1530	1550	1554	1545	1575	1553	1568
CH ₃	1419	1438	1455	1422	1407	1429	1440
C-O-C	1072	1066	1074	1067	1070	1068	1064
N-H	750-650	743-687	717-738	737-658	685	742-673	737-657

*Puspawati and Dan Simpen (2010)

Table 5: Wavelength of the main bands obtained for the extracted chitin from six different beetles.

Vibrational modes	α standard chitin (cm ⁻¹)*	<i>Oryctes Rhinoceros</i> (cm ⁻¹)	<i>Abscondita Perplexa</i> (cm ⁻¹)	<i>Lanelater Species</i> (cm ⁻¹)	<i>Holotricha serrata</i> (cm ⁻¹)	<i>Anamola Bengalensis</i> (cm ⁻¹)	<i>Anamola Varicolor</i> (cm ⁻¹)
OH out-of-plane bending	690	687	658	691	685	673	689
NH out-of-plane bending	752	744	738	761	774	742	738
Ring stretching	896	896	894	897	894	898	904
CH ₃ wagging along chain	952	952	947	958	950	956	946
CO stretching	1026	1025	1029	1027	1028	1029	1022
Asymmetric in-phase ring stretching mode	1116	1113	1312	1110	1119	1111	1095
CH ₂	1418	1438	1379	1422	1407	1429	1440

The Extraction and Characterisation of Chitin and Chitosan from Six Species of Beetles: Demonstrate That Beetles Are a Valuable Source of These Biopolymers

bending and CH ₃ deformation							
Amide II band	1563	1550	1554	1546	1575	1553	1568
Amide I band	1661	1631	1654	1650	1655	1651	1663
CH stretching	2878	2865	2845	2853	2879	2878	2890
Symmetric CH ₃ stretching and asymmetric CH ₂ stretching	2930	2948	2977	2937	2932	2938	2928
NH stretching	3268	3257	3260	3270	3266	3264	3266
OH stretching	3439	3447	3412	3431	3438	3426	3433

*α chitin standard (Palpandi *et al.*, 2009)

The FTIR spectra of chitosan obtained for six species of beetles (Figure 6A-F), (Table 6) showed the following characteristic peaks at 3450 cm⁻¹ (standard): absorption bands due to O-H stretch, 3433, 3444, 3451, 3459, 3439, 3428, 2891-2901, at wave length 3335 cm⁻¹ (standard) N-H stretching 3349, 3307, 3331, 3318, 3342, 3326, and at the peak 2891 for revealing C-H stretching 2875, 2869, 2851, 2882, 2880, 2883 by the chitosan derived from the species *Oryctus rhinoceros*, *Abscondita perplexa*, *Lanelater* species,

Holotrichia serrata, *Anomala bengalensis*, and *Anomala varicolor*, respectively. The NH₂ cutting, N-H bending, CH₃, and H group peaks with their respective peak values are presented in Table (6).

The degree of deacetylation of chitosan determined for each of the six species was as follows *Oryctus rhinoceros* 69.54%, *Abscondita perplexa* 69.3%, *Lanelater* species 69.37%, *Holotrichia serrate* 69.4%, *Anomala bengalensis* 69.33% and *Anomala varicolor* 69.31%. (Table. 7)

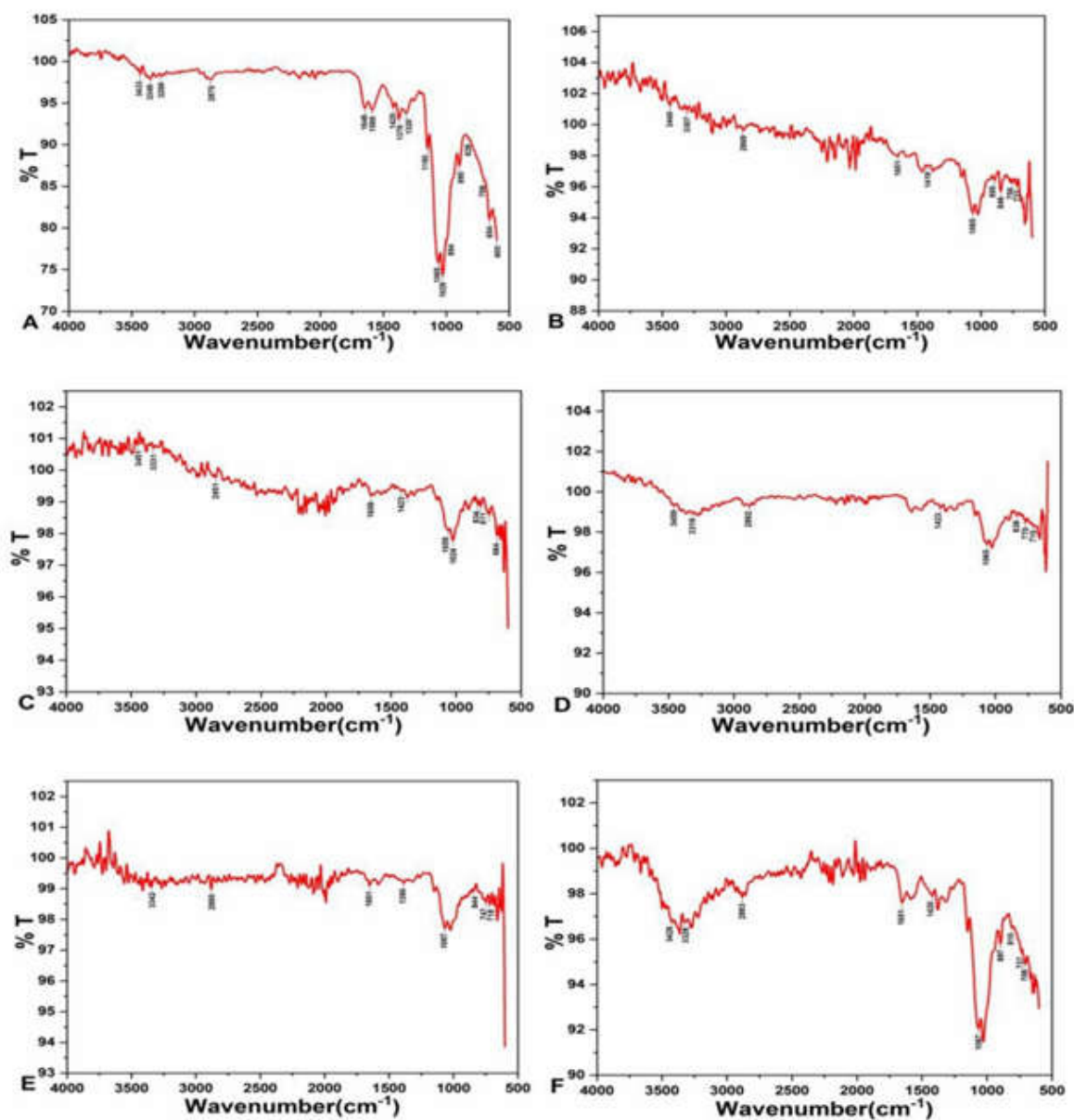


Figure 6: FT-IR spectra of chitosan from A. *Oryctes rhinoceros*, B. *Abscondita perplexa*, C. *Lanelater species*, D. *Holotrichia serrata*, E. *Anomala bengalensis*, F. *Anomala varicolar*

The Extraction and Characterisation of Chitin and Chitosan from Six Species of Beetles: Demonstrate That Beetles Are a Valuable Source of These Biopolymers

Table 6: Functional groups of extracted chitosan from six different beetles compared with commercial standard chitin

Groups	Wavelength(cm ⁻¹)						
	*Commercial std chitosan	<i>Oryctes rhinoceros</i>	<i>Abscondita perplexa</i>	<i>Lanelater species</i>	<i>Holotricha serrata</i>	<i>Anomala bengalensis</i>	<i>Anomala varicolor</i>
OH	3450.0	3433	34440	3451	3459	3439	3428
N-H stretching	3335.0	3349	3307	3331	3318	3342	3326
C-H stretching	2891.1	2875	2869	2851	2882	2880	2883
NH2 cutting, N-H bending	1655.0	1648	1651	1656	1641	1651	1651
CH3	1419.5	1420	1419	1423	1423	1390	1420
C-O-C	1072.3	1065	1065	1059	1065	1067	1067
NH2	850.0-750.0	828	846-758	834-811	838-770	844	810-737
N-H	715.0	708	721	684	715	718	708

*Puspawathi and Dan Simpen(2010)

Table 7: Percent of Degree of deacetylation of chitosan (calculation)

Species Name	Absorbance peak A1320	Absorbance peak A1420	Calculated DA	DDA(100-DA)%
<i>Oryctes rhinoceros</i>	93.709	94.422	30.457	69.543
<i>Abscondita perplexa</i>	97.29	97.33	30.685	69.3
<i>Lanelater species</i>	99.147	99.368	30.627	69.37
<i>Holotrichia serrate</i>	99.091	99.214	30.653	69.4
<i>Anomala bengalensis</i>	99.204	99.268	30.67	69.33
<i>Anomala varicolor</i>	99.844	97.868	30.625	69.37

DISCUSSION

Insects constitute a substantial reservoir of chitin and chitosan (Hahn et al., 2020), and the extraction of these biomolecules from insect biomass offers enormous worldwide advantages (Mohan et al., 2020). Nevertheless, there is limited knowledge regarding the physicochemical characteristics of these compounds in insects (Shin et al., 2019). Biopolymers such as chitin and chitosan are essential for various industrial applications in the fields of biotechnology, agriculture,

medicine, and food. Given the substantial demand, it is imperative to seek for alternative sources for these biomolecules. Assessing the feasibility of using beetles as a means to create chitin and chitosan becomes a top focus. Comparatively extraction of these molecules from insects is easier. The technique of extracting chitin and chitosan from insects involves several steps, including demineralization, deproteinization and deacetylation. Most researchers (Mei et al., 2024) favor this chemical method for chitosan production in insects compared to other options

due to its simplicity and cost-effectiveness. The current investigation found that the chitin yield, relative to dry mass, varied from 7.2% in *Anomala bengalensis* to 42% in *Holotrichia serrata*. This was followed by 35.9% in *Oryctus rhinoceros*, 33.2% in *Lanelater* species, 22.9% in *Abscondita perplexa*, and 14.9% in *Anomala varicolor*. Several reports on the extracted chitin content of different insect groups were found to be between 15% and 20% in general (Mei et al., 2024); in grasshoppers, between 20.5% and 16.5%; in silkworms, *Bombyx mori*, 15-20% (Zhang et al., 2000); in cicada sloughs, it was about 36% (Sajomsang and Gonil, 2009); and, in Cockroaches the yield of chitin ranged between 13 and 18% (Kaya and Baran, 2015). The chitin content also varies in different stages of development, such as larva, pupa, and adults. (Kaya et al., 2016; Wang et al., 2020). In crustacean shell, with the involvement of several investigations, the chitin extract differed from 7-40% (Tolaimate et al., 2003). In contrast to the other species examined, the six beetle species analyzed in this study exhibit a high chitin yield, making them a potentially viable alternative source for chitin production. Out of the six species mentioned, four of them are scarabid tunneller beetles. These beetles can be readily cultivated and taken care of by placing them under a pile of decomposing grass or animal dung. The *Lanelater* species primarily inhabits the subterranean layer of soil, the humus. In contrast, *Abscondita perplexa*, the firefly, necessitates distinct tactics for its maintenance due to its unique natural habitat.

The yield of chitosan derived from chitin varies among different species of insects. For example, it can be as low as 3.1% in the chrysalis of *Bombyx mori* (Hahn et al., 2020), or as high as 95.9% in *Clanis bilineata* (Kaya et al., 2017). In certain insects like *Leptinotarsa decemlineata*, the chitosan yield ranges from 7% to 20% between the larval stage and adulthood (Saman et al., 2014). In *Hermetia illucens*, different researchers have reported a wide variation in chitosan yield, ranging from 3.1% to 81% (Teo et al., 2022; Triunfo et al., 2022). The chitosan derivation in beetles varies across different developmental stages; in the beetles *Tenebrio molitor* and *Zophobas mario*, the larval stage produced 80% chitosan, while adults yielded chitosan ranging

from 78% to 75.63%. Super worms yielded chitosan ranging from 75% to 83.33% (Nafary et al., 2023[34]). In the rhinoceros beetle *Allomyrina dichotoma*, the chitosan derived was approximately 83.37% in both the larval and pupal stages, and 75% in the adult stage (Nafary et al., 2023). The study exclusively utilized adult insects to extract chitosan, with chitosan yields ranging from 13.5% in *Anomala varicolor* to 89.2% in *Abscondita perplexa*. The other three tunneller beetles had chitosan yields ranging from 24.9% to 41.57%, which is considered a favorable yield. This study has conducted a comparison of the amount of chitosan produced in relation to the amount of chitin extracted, as well as in connection to the dry weight of the raw material. Conversely, the variability in chitosan yield in relation to the dry weight of raw material can assist in the selection of beetle species for large-scale production in their cultivation, if one is specific to such selection.

The scanning electron microscopy (SEM) pictures have revealed distinct variations in the structural characteristics across all six species of beetles examined. The external structure of chitin differs among different species. Nanofibers and nanopores have been discovered in crustaceans and insects (Mushi et al., 2014; Yen et al., 2009). In their study, Kaya et al. (2014) discovered the presence of non-porous nanofibres on certain chitin surfaces, while other surfaces exhibited porous nanofibres [Kaya M. and Sargin I. (2016), Kaya M, et al (2016a), Kaya, et al (2015)]. The chitin morphology in *Cydalima perspectalis* (Kilci et al., 2024) showed variances among different body sections and areas. The chitin morphology of insects varies both among species and different body parts, indicating that there is no universally standardized morphology for alpha-chitin. Chitin-binding proteins commonly engage with chitin fiber bundles to generate more complex arrangements. The fibrous extracellular matrix in arthropods' cuticles is primarily composed of chitin laminae. These sheets consist of α -chitin crystals, β -folded proteins, and chitin fibers that intersect at right angles. The configuration of these clusters dictates the precise morphology of chitin (Moussain, 2019).

The Extraction and Characterisation of Chitin and Chitosan from Six Species of Beetles: Demonstrate That Beetles Are a Valuable Source of These Biopolymers

The qualities of chitin and chitosan are determined by their surface morphology. The porous nature of chitin allows for effective absorption of metal ions, making it valuable in tissue engineering applications (Arnaz et al., 2009). The fibrillar structure of chitosan is beneficial in the textile industries (Synowiecki and Al-Khateeb, 2003). The current study observed various surface morphologies of chitin and chitosan. Chitin exhibited a smooth laminar structure with nano pores and nanofibers. It also displayed flake-like structures with a rough surface, characterized by irregular nanofibers. Additionally, chitin flakes were found to have lamellar structures and entangled nanofibers between smooth surface flakes. Furthermore, smallflake-like structures with both rough and smooth surfaces were observed, along with chitin flakes that had depressions and distinct scattered nanofibers. These characteristics demonstrate the variety of chitin patterns found in different beetle species. The chitosan in all six species of beetles exhibited a consistent flake-like appearance, while the specific characteristics of the flakes varied across the different species. The lamina consisted of uneven, abbreviated nanofibers, similar to those found in *Oryctus rhinoceros*, and contained small, thinly distributed nanopores. The chitosan material is porous and contains uniformly distributed bundles of nanofibers in *Abscondita perplexa*. In *Anomala varicolor*, chitosan is organized into dense clusters of nanofibers that are aligned in parallel. Within this particular species, chitosan is present in the form of irregular flakes with uneven forms, as well as thick bundles of irregular nanofibers. Several of the chitosan flakes exhibited a prominent concave area in their center. These findings indicate that the chitosan found in these six species of beetles differs significantly from that found in other insects in various characteristics.

The degree of crystallinity plays a crucial role in determining the various properties of polymers and also helps in comprehending their supra molecular arrangements. We evaluated the crystallinity of chitin and chitosan by comparing the heights of their crystalline and amorphous scattering diffraction peaks at specific angles- 12°, 12.6°, and 16°. Analyzing the crystalline nature of chitin and chitosan using X-ray

diffraction (XRD) is vital for understanding their molecular configurations and levels of crystallinity. We employed the widely used XRD technique to reveal the structure of these molecules, resulting in distinct peak patterns that indicate the presence of crystalline regions within the molecules. Chitin from all six species of beetles displayed well-defined peaks, indicating a highly ordered molecular structure. Chitosan, with its partially deacetylated structure, produced broader and less intense peaks, suggesting a less orderly arrangement compared to chitin. XRD analysis allows for the determination of the degree of crystallinity, providing insights into the relative quantity of crystalline and amorphous regions. Greater crystallinity signifies a more organized molecular structure, whereas lower crystallinity indicates a disordered or amorphous nature of the molecule.

In the present study the chitin of *Oryctus rhinoceros* generated two high peaks at 9.2°, 19.2°, 22.8°, 26.3° degrees, *Abscondita perplexa* produced high peaks at 9.2°, 19.2°, 24.1°, 26.22° degrees, similarly the click beetle *Lanelater* species had borne high peaks 9.2°, 19.3°, 23.5°, 26.5°, *Holotricha serrata* had high peaks at 9.2°, 19.3°, 23.6°, 26.3°, *Anomala bengalensis* and *Anomala varicolor* too generated high peaks at 9.2°, 19.3°, 23°, 26.5° and 8.7°, 20°, 23°, 26.3° degrees respectively. The XRD analysed samples of other insects have shown similar peaks between 4° and 25°, around 9.4°; 13.0°; 19.3°; 20.8°, 23.2°, and 29.5° and the same peaks were found in the commercial shrimp sample 9.4°; 12.9°; 19.4°; 20.9° and 23.6°. Similar works in a few species insects of such as Mealworm (Luo et al., 2019), *Omophlus sp.* (Kaya et al., 2016[31]), Cockchafer, *Melolontha melolontha* (Kaya et al., 2014), Cockchafer, *Melolontha sp.* (Kaya et al., 2017), Kaya et al., 2014), *Calosoma rugosa* (Marie et al., 2019), Rhinoceros beetle, *Allomyrina dichotoma* (Shin et al., 2019), Colorado potato beetle, *Leptinotarsa decemlineata* Larvae (Saman et al., 2014). European stag beetle, *Lucanus cervus* (Kabalak et al., 2020) Pine chafer, *Polyphylla fullo* Wheat weevil, *Sitophilus granaries* (Jagdale et al., 2022) Dor beetle, *Anoplotrupes stercorosus* (Kaya et al., 2016[28]) *Blaps tibialis*, *Cetonia aurata*, *Geotrupes stercorarius*, *Blaps lethifera* (Amor et al., 2023)

have shown the peak formation in the same area indicate the universality of this feature in chitin molecule of insects.

Fourier transform infrared spectroscopy (FTIR) is a technique that can be employed to examine the chemical composition of a sample by producing a spectrum that reveals the specific wavelengths at which the sample absorbs infrared light. This is possible because each organic molecule possesses a distinct infrared resonance frequency.

The major bands of insect-based chitin and chitosan occur at specific wave numbers corresponding to CN stretching, amide III (1310–1320 cm⁻¹), NH bending, amide II (1550–1560 cm⁻¹), NH₂ bending (1590–1600 cm⁻¹), CO stretching, amide I (1650–1655 cm⁻¹), NH symmetric stretching (3100–3110 cm⁻¹), NH asymmetric stretching (3255–3270 cm⁻¹), and OH stretching (3430–3450 cm⁻¹), based on the functional groups present in the molecules. For insect-based chitin and chitosan, infrared spectra were used to confirm the consistency of the chitin and chitosan obtained from different insect species, compare the spectral bands with those of commercially available chitin and chitosan, and assess the purity of insect-based chitin after isolation by examining the strength and position of characteristic bands.

The Fourier Transform Infrared (FTIR) spectra were obtained for chitin extracted from six different species of beetles showed a characteristic pattern. The chitin exhibited a characteristic band at 3257, 3260, 3270, 3266, and 3466 cm⁻¹, indicating the presence of N-H asymmetric stretching. The bands observed at 3447, 3412, 3431, 3438, 3426, and 3433 cm⁻¹ correspond to the stretching vibration of hydroxyl (OH) groups. On the other hand, the bands at 2865, 2845, 2853, 2879, 2878, and 2890 cm⁻¹ represent aliphatic carbon-hydrogen (C-H) stretching bands that overlap with the OH stretching bands in the presence of nitrogen-hydrogen (N-H) for the species *Oryctus rhinoceros*, *Abcondita perplexa*, *Lanelater species*, *Holotrichia serrata*, *Anomala bengalensis*, and *Anamola varicolor*. The characteristic carbonyl C = O stretching of chitin at 1025, 1029, 1027, 1028, 1029, and 1022 cm⁻¹, as well as at 1550, 1554,

1546, 1575, 1553, and 1568 cm⁻¹, is attributed to the vibrations of the amide I band. The presence of a distinct peak at 1438, 1379, 1422, 1407, 1429, and 1440 cm⁻¹ indicates the occurrence of asymmetrical deformation. The distinct peak observed at 1550, 1554, 1546, 1575, 1553, and 1568 cm⁻¹ corresponds to the N-H deformation of amide II. The characteristic carbonyl C = O stretching of chitin at 1025, 1029, 1027, 1028, 1029, and 1022 cm⁻¹, as well as at 1550, 1554, 1546, 1575, 1553, and 1568 cm⁻¹, is attributed to the vibrations of the amide I band, that has been discussed by other researchers. The CH₃ group exhibits asymmetrical deformation, which is indicated by the distinct peaks observed at 1438, 1379, 1422, 1407, 1429, and 1440 cm⁻¹. The N-H deformation of amide II is indicated by the distinct peak observed at 1550, 1554, 1546, 1575, and 1553. The C-O-C vibrations within the chitin ring were seen at specific frequencies of 1438, 1455, 1422, 1407, 1429, and 1440 cm⁻¹ in the six beetles mentioned above, in the correct sequence. The presence of hydroxide from chitin, which contains a single bond C = O, resulted in the formation of several peaks in these bands (Puspawati and Dan Simpen, 2010; Palpandi *et al.*, 2009). The majority of insects examined in published studies have been identified to have only α -chitin, and the α -chitin of *Melolontha melolontha* (Kaya *et al.*, 2017), several grasshoppers (Jaworska *et al.*, 2003, D'Hondt *et al.*, 2020, the potato beetle (Hahn *et al.*, 2020), and crickets (Peng *et al.*, 2022), the larvae and flies of the black soldier fly (Waśko *et al.*, 2016) possess α -chitin and have nearly identical FTIR band patterns.

Chitosan of beetles displayed a broad absorption band in the range 3459 - 3428 cm⁻¹ which is attributed to O-H stretching vibrations and the 3349 - 3318 cm⁻¹ to vibration of NH. The stretching vibrations of methylene C-H at 2854 cm⁻¹, absorption peak at 1558 cm⁻¹ correspond to the NH₂. The amide II band is used as the characteristic band of N-acetylation (Islam *et al.*, 2011). The spectra of chitosan showed the different vibration that occurs after deacetylation process, which was not the emergence of vibration C = O at 1065 - 1067 cm⁻¹ region, which indicates the vibration of C = O has been reduced on chitosan, It confirms the

The Extraction and Characterisation of Chitin and Chitosan from Six Species of Beetles: Demonstrate That Beetles Are a Valuable Source of These Biopolymers

presence of N-acetylglucosamine units in the chitin structure.

The main goal of studies on chitosan is to make it suitable for use in various fields of biology and medicine, depending on its degree of deacetylation. In this study was done by calculating the ratio of absorbance of the Amide III at 1320 cm⁻¹ to the absorbance of the CH₃ bending at 1420 cm⁻¹. The obtained values by this method were found to be consistent with values obtained by other procedures (Joydeep Dutta and Priyanka in 2022). The level of deacetylation influences the solubility of chitosan; as its crystallinity remains higher, it becomes less soluble and more rigid. This retained rigidity of chitosan boosts its mechanical strength, making it ideal for creating platforms for tissue engineering, medical, cosmetic, and pharmaceutical sectors (Sajomsang and Gonil 2009). Insect-derived chitosan, in general, can have a deacetylation degree ranging from 62% to 98% (Hahn et al., 2020). By varying the degree of deacetylation, one can change the biological functions of chitosan, such as its ability to stimulate the immune system, heal wounds, and prevent the growth of cancer and inflammation. In this study of six beetle species samples, chitosan's DDA was slightly more than 69% in all the species, which may have an impact on the material's solubility and possible applications in tissue engineering and pharmaceuticals.

CONCLUSION

Presently, the investigation of chitin is becoming increasingly important, and chitosan, a by-product of chitin, is widely employed by academics and industrial makers for diverse applications. There is a growing need to manufacture chitin from various sources. In order to fulfil this requirement, researchers are actively exploring insects as highly promising sources of these biopolymers. This study involved the examination of many types of beetles, with a specific emphasis on scarabid beetles, which possess the ability to generate significant amounts of chitin. Beetles constitute a substantial quantum of insects in terms of biomass and have the potential to be explored for large-scale cultivation. This study has

revealed, the extraction of chitin and chitosan may be done using a straight forward approach and characterization of these substances can be analyzed using commonly used techniques such as XRD, FTIR, and SEM examination.

Authors' contributions

All the authors made equal contributions to this work. SSA and SS collected the insects as well carried out chemical extraction of molecules, NSD and SV assisted in characterization of molecules, HC designed the work plan and interacted at all phases of the work. All the authors are involved in preparing the manuscript.

Acknowledgement

Authors are thankful Institute of excellence, University of Mysore for providing SEM, XRD, FTIR facilities to carry out this work successfully. We extend our thanks to Head of department of studies in Zoology, Manasa gangotri, UoM, Mysuru for encouraging this programme.

Competing interests

There is no competing interest involved in this research.

Funding

This research is not supported by any kind of funds.

REFERENCES

- Abidin, N. A. Z., F. Kormin, N. A. Z. Abidin, N. A. F. Mohamed Anuar and M. F. Abu Bakar. (2020). The potential of insects as alternative sources of chitin: An overview on the chemical method of extraction from various sources. *International Journal of Molecular Sciences*. 21, 4978.
- Amor I. B., Hemmami H., Laouini S. E., Abdelaziz A. G., and Barhoum A. (2023). Influence of chitosan source and degree of deacetylation on antibacterial activity and adsorption of AZO dye from water. *Biomass Conversion and Biorefinery*, 1–11. 10.1007/s13399-023-03741-9

- Aranaz, I.; Mengibar, M.; Harris, R.; Paños, I.; Miralles, B.; Acosta, N.; Galed, G. & Heras (2009). Characterization of Chitin and Chitosan. *Current Chemical Biology*, 3, 203–230, pISSN1872-3136
- Hahn, T., Tafi, E., Paul, A., Salvia, R., Falabella, P., and Zibek, S. (2020). The current state of chitin purification and chitosan production from insects. *Journal of Chemical Technology & Biotechnology*, 95, 2775–2795. doi: 10.1002/jctb.6533
- Dahmane EM, Taourirte M, Eladlani N, et al. (2014): Extraction and characterization of chitin and chitosan from *Parapenaeus longirostris* from Moroccan local sources. *International journal of polymer analysis and characterization*, 19(4):342–351.
<https://doi.org/10.1080/1023666X.2014.902577>
- D'Hondt, E., Soetemans, L., Bastiaens, L., Maesen, M., Jespers, V., van den Bosch, B., et al. (2020). Simplified determination of the content and average degree of acetylation of chitin in crude black soldier fly larvae samples. *Carbohydrate Research*. 488:107899. doi: 10.1016/j.carres.2019.107899
- El Knidri, H., R. Belaabed, A. Addaou, A. Laajeb and A. Lahsini. (2018). Extraction, chemical modification and characterization of chitin and chitosan: A review. *International Journal of Molecular Sciences* 120(Part A): 1181–1189
- Elkadaoui S, Azzi M, Desbrieres J, Zim J, El Hachimi Y, Tolaimate A. (2024). Valorization of *Hermetia illucens* breeding rejects by chitins and chitosans production. Influence of processes and life cycle on their physicochemical characteristics. *International Journal of Biological Macromolecules*. May; 266(2), 131314. doi: 10.1016/j.ijbiomac.2024.131314.
- Hajji S., Younes I., Ghorbel-Bellaaj O., et al. (2014). Structural differences between chitin and chitosan extracted from three different marine sources. *International Journal of Biological Macromolecules*, 65:298–306. <https://doi.org/10.1016/j.ijbiomac.2014.01.045>
- Islam, M. M., Masum, S. M., Rahman, M. M., Molla, M. A. I., Shaikh, A. A., & Roy, S. K. (2011). Preparation of chitosan from shrimp shell and investigation of its properties. *International Journal of Basic and Applied Sciences*, 11(1), 77–80.
- Jagdale, P.; Mharsale, N.; Gotarne, R.; and Magdum, S. (2022) Extraction and Characterization of Chitin from Granary Weevil, *Sitophilus granaries* L. (Coleoptera: Curculionidae). *Arthropods*, 11, 176–185.
- Jang, M., Kong, B., Jeong, Y., Lee, C.H., & Nah, J.W. (2004). Physicochemical characterization of α -chitin, β -chitin, and γ -chitin separated from natural resources. *Journal of Polymer Science Part A*, 42, 3423–3432.
- Jaworska M, Kensuke Sakurai, Pierre Gaudon, Eric Guibal (2003). Influence of chitosan characteristics on polymer properties. I: Crystallographic properties. *Polymer International*, 52(2), 198–205.
<https://doi.org/10.1002/pi.1159>
- Joydeep Dutta, Priyanka. (2022). A facile approach for the determination of degree of deacetylation of chitosan using acid-base titration. *Heliyon* 8 (2022) e09924
- Kabalak M., Aracagök D., and Torun M. (2020): Extraction, characterization, and comparison of chitins from large-bodied four Coleoptera and Orthoptera species. *International Journal of Biological Macromolecules*, 145:402–409.
- Kavya, M. K., Raghunandan, K. S., Padmanabha, B., and Channaveerappa, H. (2018). Comparative scanning electron microscopic study of antennae and hearing organs of two Indian mantids, *Mantis religiosa* and *Gongylus gongylodes*. *International Journal of Zoological Investigations*, 4 (1): 73–80
- Kaya M. and Sargin I. (2016). Highly fibrous and porous raw material-shaped chitin was isolated from *Oniscus* sp. (Crustacea). *Food Biophysics* 11:101–107
- Kaya M., Sargin I., Al-Jaf I., Erdogan S., and Arslan G. (2016a). Characteristics of corneal lens chitin in dragonfly compound eyes. *International*

- Journal of Biological Macromolecules*, 89, 54-61. doi: 10.1016/j.ijbiomac.2016.04.056. Epub 2016 Apr 22. PMID: 27109757
- Kaya M., Baublys V., Can E., Šatkauskienė I., Bitim B., Tubelytė V., et al. (2014) Comparison of physicochemical properties of chitins isolated from an insect (*Melolontha melolontha*) and a crustacean species (*Oniscus asellus*) *Zoomorphology*. ; 133(3), 285–293.
- Kaya M., Sargin I., Sabeckis I., Noreikaite D., Erdonmez D., Salaberria A.M., and Tubelytė V. (2017), Biological, mechanical, optical, and physicochemical properties of natural chitin films obtained from the dorsal pronotum and the wing of cockroaches, *Carbohydrate Polymers*, 163:162-169.
- Kaya, M.; Baran, T. (2015). Description of a new surface morphology for chitin extracted from the wings of cockroaches (*Periplaneta americana*). *International Journal of Biological Macromolecules*. 75, 7-12.]
- Kaya, M.; Sofi, K.; Sargin, I.; Mujtaba, M. (2016b). Changes in Physicochemical Properties of Chitin at Developmental Stages (Larvae, Pupa, and Adult) of *Vespa Crabro* (Wasp). *Carbohydrate Polymers*, 145, 64-70.
- Kaya, M., E. Lelešius, R. Nagrockaite, I. Sargin, G. Arslan, A. Mol, T. Baran, E. Can, and B. Bitim (2015), Differentiations of Chitin Content and Surface Morphologies of Chitins Extracted from Male and Female Grasshopper Species, *PLoS One* 10, <https://doi.org/10.1371/journal.pone.0115531>
- Kilcy L., Nurver Altun Şengül Alpay Karaoğlu, Tugce Karaduman Yesildal (2024). Characterization of chitin and description of its antimicrobial properties obtained from *Cydalima perspectalis* adults (*Polymer Bulletin*, 10.1007/s00289-024-05)
- Kumari S., Rath P., Kumar ASH, et al. (2015). Extraction and characterization of chitin and chitosan from fishery waste by chemical method. *Environmental Technology & Innovation* 3:77–85. <https://doi.org/10.1016/j.eti.2015.01.002>
- Lavertu, M., Xia, Z., Serreqi, A. N., Berrada, M., Rodrigues, A., Wang, D., Buschmann, M. D., and Gupta, A. (2003). A validated ¹HNMR method for the determination of the degree of deacetylation of chitosan, *Journal of Pharmaceutical and Biomedical Analysis*, 32 (6), 1149–1158
- Luo, Q., Wang, Y., Han, Q., Ji, L., Zhang, H., Fei, Z., & Wang, Y. (2019). Comparison of the physicochemical, rheological, and morphologic properties of chitosan from four insects. *Carbohydrate Polymers*, 209, 266–275. <https://doi.org/10.1016/j.carbpol.2019.01.030>.
- Marei N., Elwahy A.H., Salah T.A., El Sherif Y., and Abd El-Samie E. (2019). Enhanced antibacterial activity of Egyptian local insects' chitosan-based nanoparticles loaded with ciprofloxacin-HCl. *International Journal of Biological Macromolecules*, 126:262-272.
- Mei Z, Kuzhir P, and Godeau G. (2024) Update on Chitin and Chitosan from Insects: Sources, Production, Characterization, and Biomedical Applications. *Biomimetics*.; 9(5):297. <https://doi.org/10.3390/biomimetics9050297>
- Mohan K, Ganesan AR, Muralisankar T, Jayakumar R, Sathishkumar P, Uthayakumar V, Chandirasekar R, Revathi N. . (2020): Recent insights into the extraction, characterization, and bioactivities of chitin and chitosan from insects. *Trends in Food Science and Technology*, Nov. 105:17–42. doi: 10.1016/j.tifs.2020.08.016. Epub 2020 Sep 4. PMID: 32901176; PMCID: PMC7471941.
- Moussian, B. (2019). Chitin: Structure, Chemistry, and Biology. In: Yang, Q., and Fukamizo, T. (eds.) Targeting chitin-containing organisms *Advances in Experimental Medicine and Biology*, vol. 1142. Springer, Singapore. https://doi.org/10.1007/978-981-13-7318-3_2
- Mushi N. E., Butchosa N., Zhou Q., and Berglund L. A. (2014). Nanopaper

- membranes from chitin-protein composite nanofibers—structure and mechanical properties. *Journal of Applied Polymer Science*, 131, 40121–40130, 10.1002/app.40121
- Muthukrishnan S., Mun. S., Noah M. Y., Geisbrecht E. R., Arakane Y. (2020) Insect cuticular chitin contributes to form and function. *Current Pharmaceutical Design*: 26(29): 3530–3545. doi:10.2174/1381612826666200523175409.
- Nafary A., Mousavi Nezhad SA, and Jalili S. (2023) Extraction and Characterization of Chitin and Chitosan from *Tenebrio Molitor* Beetles and Investigation of Their Antibacterial Effect Against *Pseudomonas aeruginosa*. *Advanced Biomedical Research*. 12, 96. doi: 10.4103/abr.abr_205_22.
- Palpandi, C., V. Shanmugam, and A. Shanmugam, 2009. Extraction of chitin and chitosan from the shell and operculum of the mangrove gastropod *Nerita (Dostia) crepidularia* Lamarck. *International Journal of Medicine and Medical Sciences*, 1(15): 198–205
- Puspawati, N.M., and Simpen, I. N. (2010). Optimasi deasetilasi kitin dari kulit udang dan cangkang kepiting limbah restoran seafood menjadi kitosan melalui variasi konsentrasi NaOH. *Jurnal Kimia*, 4 (1). Hal 79-90.
- Pellis A, Guebitz GM, and Nyanhongo GS. (2022) Chitosan: Sources, Processing, and Modification Techniques. *Gels*. 8(7), 393. doi: 10.3390/gels8070393.
- Peng T.H., L.K. Wei, E.C.W. Chiang, M.S.O. (2022) Yoon Antibacterial properties of chitosan isolated from the black soldier fly, *Hermetia illucens*. *Sains Malaysiana*, 51, pp. 3923–3935, 10.17576/jsm-2022-5112-05.
- Rinaudo, M. (2006). Chitin and chitosan: properties and applications. *Progress in Polymer Science*, 31, 603–632.
- Sajomsang W., Gonil P. (2009). Preparation and characterization of α -chitin from cicada sloughs. *Materials Science and Engineering*. 30, 357–363. doi: 10.1016/j.msec.11.014.
- Saman I., Menteş A., Cakmak Y.S., Baran T., Kaya M. (2014), and Asan Ozusaglam M. Physicochemical Characterization of Chitin and Chitosan Obtained from Resting Eggs of *Ceriodaphnia Quadrangula* (Branchiopoda: Cladocera: Daphniidae), *The Journal of Crustacean Biology*, 34, 283–288. doi: 10.1163/1937240X-00002221.
- Sen, M., Taskin, P., Ulanski, P., Czechowska-Biskup, R., Rosiak, J.M., Raimond, L. Al-Assaf, S. 2016. Determination of the Degree of Deacetylation of Chitosan using Various Techniques. Chapter 7, in *The Radiation Chemistry of Polysaccharides*, Al-Assaf, Saphwan; Coqueret, Xavier; Khairul Zaman, Haji Mohd Dahlan; Sen, Murat; Ulanski, Piotr (eds.); International Atomic Energy Agency, Vienna (Austria)
- Shin C.-S., Kim D.-Y., and Shin W.-S. (2019); Characterization of chitosan extracted from Mealworm Beetle (*Tenebrio molitor*, *Zophobas morio*) and Rhinoceros Beetle (*Allomyrina dichotoma*) and their antibacterial activities. *International Journal of Biological Macromolecules*, 125:72–77.
- Synowiecki, J., and Al-Khateeb, N.A. (2003). Production, Properties, and Some New Applications of Chitin and Its Derivatives. *Critical Reviews in Food Science and Nutrition*, 43, 145–171, pISSN 1040-8398
- Teo, H.P.; Law, K.W.; Eric Chan, W.C.; Michelle Soo, O.Y. (2022) Antibacterial Properties of Chitosan Isolated from the Black Soldier Fly, *Hermetia illucens*. *Sains Malays.*, 51, 3923–3935.
- Tolaimate, A., J. Desbrières, M. Rhazi, and A. Alagui. (2003). Contribution to the preparation of chitins and chitosans with controlled physico-chemical properties, *Polymer*. 44: 7939–7952. DOI: 10.1016/j.polymer.2003.10.025
- Triunfo, M.; Tafi, E.; Guarnieri, A.; Salvia, R.; Scieuzo, C.; Hahn, T.; Zibek, S.; Gagliardini, A.; Panariello, L.; Coltelli, M.B.; et al. (2022). The characterization of chitin and chitosan derived from *Hermetia illucens* is a further step in the circular economy process. *Scientific*

- Reports* 12, 6613:
<https://doi.org/10.1038/s41598-022-10423-5>
- Uğurlu, E, Önder Duysak. (2022.) A study on the extraction of chitin and chitosan from the invasive sea urchin *Diadema setosum* from Iskenderun Bay in the Northeastern Mediterranean. *Environmental Science and Pollution Research*.
<https://doi.org/10.1007/s11356-022-23728-9>
- Varma R, Vasudevan S (2020). Extraction, characterization, and antimicrobial activity of chitosan from horse mussel *Modiolus*. *ACS Omega* 5(32), 20224–20230.
<https://doi.org/10.1021/acsomega.0c01903>
- Vino AB, Ramasamy P, Shanmugam V, et al. (2012). Extraction, characterization, and in vitro anti-oxidative potential of chitosan and sulfated chitosan from the cuttlebone of *Sepia aculeata* Orbigny 1848. *Asian Pacific Journal of Tropical Biomedicine* 2(1), 334–341. [https://doi.org/10.1016/S2221-1691\(12\)60184-1](https://doi.org/10.1016/S2221-1691(12)60184-1)
- Wang, H.; Rehman, K.U.; Feng, W.; Yang, D.; Rehman, R.U.; Cai, M.; Zhang, J.; Yu, Z.; Zheng, L. (2020). Physicochemical Structure of Chitin in the Developing Stages of Black Soldier Fly. *Int. J. Biol. Macromol.*, 149, 901–907. [CrossRef] [PubMed]
- Waśko, A., Bulak, P., Polak-Berecka, M., Nowak, K., Polakowski, C., and Bieganski, A. (2016). The first report of the physicochemical structure of chitin was isolated from *Hermetia illucens*. *Int. J. Biol. Macromol.* 92, 316–320. doi: 10.1016/j.ijbiomac.2016.07.038
- Yadav M., Goswami P., Paritosh K. V., Manish Kumar, N. Pareek, and V. Vivekanand (2019). Seafood waste is a source for the preparation of commercially employable chitin and chitosan materials. *Bioresources and Bioprocessing* 6(1):1–20. <https://doi.org/10.1186/s40643-019-0243-y>
- Yen M. T., Yang J. H., and Mau J. L. (2009) Physicochemical characterization of chitin and from crab shells *Carbohydrate Polymers*, 75 (15–21)
- Yeul, V.S.; Rayalu, S.S. (2012). Unprecedented Chitin and Chitosan: A Chemical Overview. *Journal of Polymers and the Environment*. 21, 606–614. [CrossRef]
- Zhang, M., Haga, A., Sekiguchi, H., and Hirano, S. (2000). Structure of insect chitin isolated from beetle larva cuticle and silkworm (*Bombyx mori*) pupa exuvia. *International Journal of Biological Macromolecules*. 27, 99–105.
